THE JOURNAL OF PHYSICAL CHEMISTRY B
A JOURNAL OF THE AMERICAN CHEMICAL SOCIETY

pubs.acs.org/JPCB

Article

Bulk Response of Carboxylic Acid Solutions Observed with Surface Sum-Frequency Generation Spectroscopy

Carolyn J. Moll, Jan Versluis, and Huib J. Bakker*

Cite This: *J. Phys. Chem. B* 2022, 126, 270−277

Read Online

ACCESS | Metrics & More | Article Recommendations | Supporting Information

ABSTRACT: We study the molecular properties of aqueous acetic acid and formic acid solutions with heterodyne-detected vibrational sum-frequency generation spectroscopy (HD-VSFG). For acid concentrations up to ∼5 M, we observe a strong increase of the responses of the acid hydroxyl and carbonyl stretch vibrations with increasing acid concentration due to an increase of the surface coverage by the acid molecules. At acid concentrations >5 M we observe first a saturation of these responses and then a decrease. For pure carboxylic acids we even observe a change of sign of the $\mathrm{Im}[\chi^{(2)}]$ response of the carbonyl vibration. The decrease of the response of the hydroxyl vibration and the decrease and sign change of the response of the carbonyl vibration indicate the formation of cyclic dimers, which only show a quadrupolar bulk response in the HD-VSFG spectrum because of their antiparallel conformation. We also find evidence for the presence of a quadrupolar response of the CH vibrations of the acid molecules.

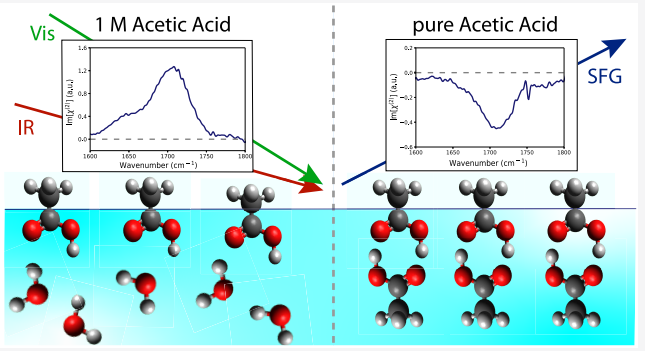

INTRODUCTION

Carboxylic acids have attracted significant attention in atmospheric chemistry in the past decades, as they are the most abundant oxygenated compounds in the atmosphere and form a major contributor to free acidity in precipitation.[1,2] Interactions of atmospheric inorganic and organic species, including carboxylic acids, play a major role in many environmental processes and are thus important in the study of climate change. Furthermore, carboxylic acids are also commonly associated with atmospheric corrosion of metal surfaces. Within the corrosion process corrosive gases like formic acid (FA) and acetic acid (AA) penetrate a thin layer of water that covers the metal and subsequently oxidize and damage the metal.[3,4] Therefore, the understanding of chemical processes at surfaces as the adsorption behavior of carboxylic acids is of great importance to atmospheric and surface chemistry.[5] Beside surface tension measurements,[6] atomic force microscopy (AFM),[7] surface-enhanced Raman scattering (SERS),[8] and X-ray photoelectron spectroscopy (XPS),[5] vibrational sum-frequency generation spectroscopy (VSFG) is a powerful tool as a probe for microscopic structures at interfaces.[9,10] VSFG is highly surface sensitive and surface selective because VSFG is based on the second-order polarization of the system, which is prohibited in centrosymmetric media and therefore in most bulk phases. Recently, many studies challenged this basic understanding of VSFG and demonstrated that sum-frequency light can also be generated by a bulk quadrupolar response.[10−14] Clearly, the presence of such a response influences the surface selectivity and interpretation of VSFG spectra.[10,13,14] Previous intensity VSFG measurements of aqueous FA and AA show that the vibrational responses of the CH, OH, and C═O vibrations of acid molecules at the surface can already be observed at low concentrations (0.3 mol %).[15−17] These studies also reported that these spectral responses change in shape upon increasing the concentration, which was explained from the formation of complexes of acid molecules, such as the hydrated monomer, the linear dimer, and the cyclic dimer. Here, we investigate the properties of FA and AA molecules at the surface of aqueous solutions with heterodyne detected vibrational sum-frequency generation (HD-VSFG). The signal measured with this technique is directly proportional to the complex second-order susceptibility $\chi^{(2)}$, whereas the signal probed in intensity VSFG is proportional to $|\chi^{(2)}|^2$. As a result, HD-VSFG provides unique information about the orientation of the molecular groups of the acid molecules at different concentrations and, as the signal is proportional to $\chi^{(2)}$ instead of $|\chi^{(2)}|^2$, HD-VSFG enables the detection of low-concentration species that in intensity VSFG measurements are overwhelmed by the response of the dominant species. By varying the acid concentration, we demonstrate the presence of both a surface

Received: October 18, 2021
Revised: December 10, 2021
Published: December 28, 2021

https://doi.org/10.1021/acs.jpcb.1c09051
J. Phys. Chem. B 2022, 126, 270−277

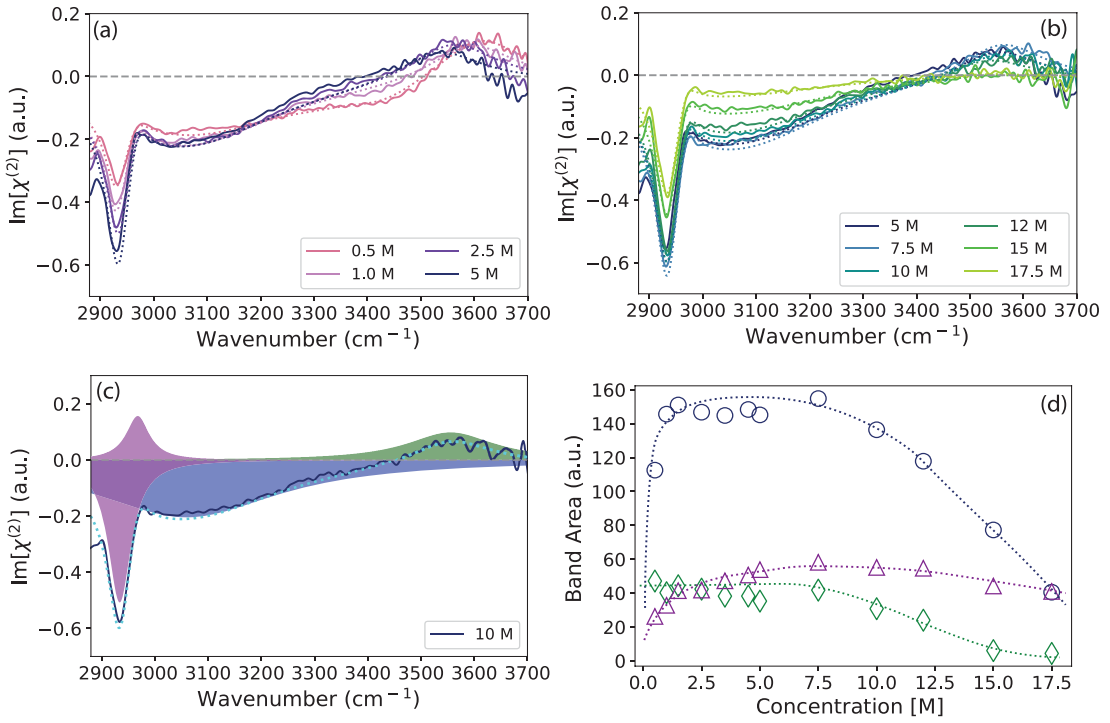

Figure 1. Im[$\chi^{(2)}$] spectra of aqueous solutions containing different concentrations of AA (a) in the range of 0.5−5 M and (b) in the range of 5−17.5 M (pure AA) in the frequency region of 2850−3700 cm^{-1}. (c) Decomposed spectra of a 10 M AA solution with four Lorentzian bands centered at 2935, 2970, 3060, and 3600 cm^{-1} describing the symmetric ($\nu_{CH_3,SS}$) and antisymmetric ($\nu_{CH_3,AS}$ stretch vibrations (magenta) and the OH stretch vibrations of the strongly (blue) hydrogen-bonded AA molecules and of the weakly hydrogen-bonded water molecules (green). (d) Absolute area of these bands extracted from the fitting procedure as a function of acid concentration.

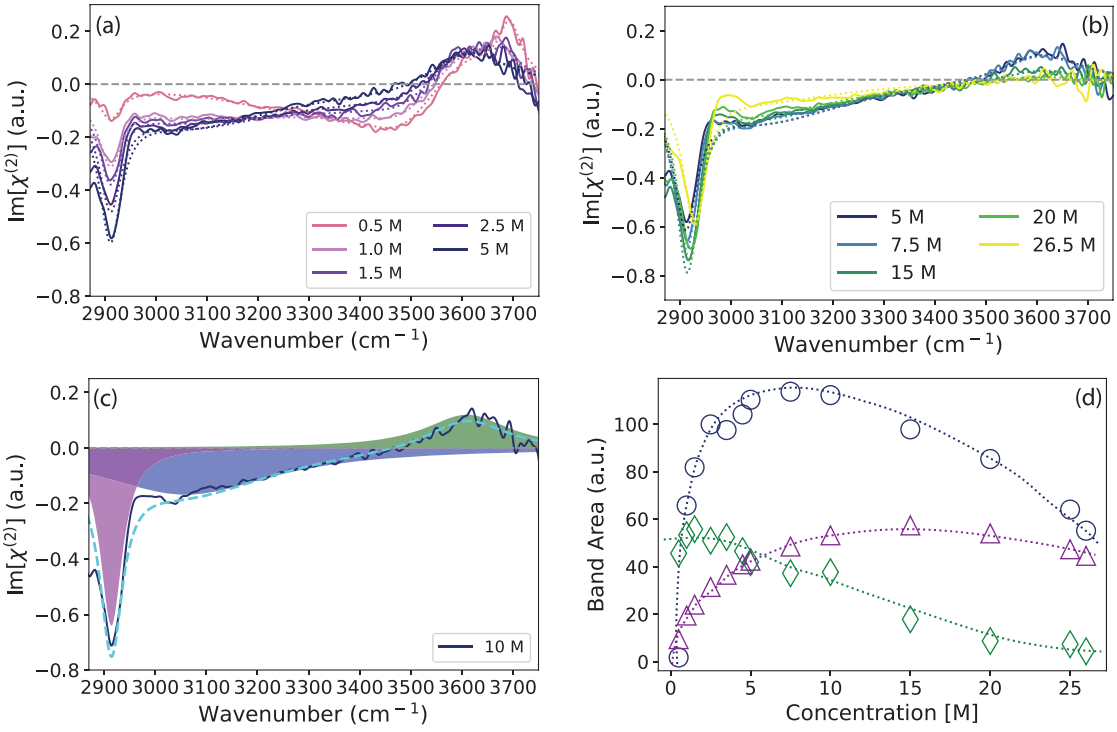

Figure 2. Im[$\chi^{(2)}$] spectra of aqueous solutions containing different concentrations of FA (a) in the range 0.5−7.5 M and (b) in the range 7.5−26.5 M (pure FA) in the frequency region of 2850−3750 cm^{-1}. (c) Decomposed spectra of FA with three Lorentzian bands centered at 2910, 3060, and 3600 cm^{-1} describing the CH stretch vibration of the methine group (magenta) and the OH stretch vibrations of the strongly (blue) hydrogen-bonded FA molecules and of the weakly hydrogen-bonded water molecules (green). (d)Absolute area of these bands extracted from the fitting procedure as a function of acid concentration.

https://doi.org/10.1021/acs.jpcb.1c09051
J. Phys. Chem. B 2022, 126, 270−277

dipolar contribution and a bulk quadrupolar contribution to the responses of the C═O and CH vibrations.

EXPERIMENTAL METHODS

In the following we describe briefly our implementation of HD-VSFG. A more detailed description of the technique can be found in previous publications.[18−21] We use an amplified Ti:sapphire laser system (1 kHz, 35 fs, 6.5 mJ/pulse) to generate a narrow 800 nm beam and a tunable, broadband mid-infrared beam. The two beams are spatially and temporally overlapped at the surface of a gold mirror to generate light at the sum-frequency that serves as a local oscillator (LO-SFG). Before the 800 nm beam (s-polarized), the IR beam (p-polarized), and the LO-SFG signal (s-polarized) are focused on the sample surface, the LO-SFG signal is sent through a silica plate to delay it in time (∼1.6 ps). The 800 nm and IR beams generate a second SFG signal at the sample surface. The SFG signal of the sample and the LO-SFG signal are sent into a spectrograph and frequency-resolved detected with a thermoelectrically cooled charged-coupled device (CCD, Princeton Instruments). From the interference spectrum of the two SFG signals the real (Re) and imaginary (Im) $\chi^{(2)}$ spectra are extracted, providing direct information about the orientation of the vibrational transition dipole moments and thus on the absolute orientation of the molecules at the surface.[18] We correct the spectra for the spectral dependence of the input IR beam by dividing the HD-VSFG spectrum of the sample by the HD-VSFG spectrum of a reference z-cut quartz crystal. To obtain high quality data in the frequency region of 1500−1750 cm^{-1}, we take two independent measurements of z-cut quartz with a different orientation of 180°. By addition of the two quartz spectra, the interference induced by the SFG signal of the local oscillator and the quartz is removed. The remaining modulation, which largely represents the structural noise on the CCD camera induced by the etaloning effect, can now be used as a scaling factor to remove the structural noise from the data.[12] For all measurements we used water from a Millipore Nanopure system (18.2 MΩ·cm). Acetic acid (99.8%) and formic acid (98%) were purchased from Sigma-Aldrich and are used without further purification. All measurements are performed with a custom-built sample cell. The sample cell is made of Teflon and can hold a sample solution with a volume up to 4 mL.

RESULTS AND DISCUSSION

In Figures 1a,b and 2a,b measured $\mathrm{Im}[\chi^{(2)}]$ spectra of aqueous AA and FA solutions at different concentrations in the frequency region 2850−3700 cm^{-1} are presented. For AA the concentration ranges from 0.5 to 17.5 M (pure) and for FA from 0.5 to 26.5 M (pure). At all concentrations the $\mathrm{Im}[\chi^{(2)}]$ spectra of the AA solutions show a narrow negative feature at 2935 cm^{-1} which we assign to the symmetric stretch vibration of the methyl group ($\nu_{CH_3,SS}$) of the AA molecule. In addition, the spectra show a narrow positive band at 2970 cm^{-1} which we assign to the antisymmetric stretch vibration of the methyl group ($\nu_{CH_3,AS}$).[16,22] For FA the $\mathrm{Im}[\chi^{(2)}]$ spectra show a single negative band in the CH region centered at 2910 cm^{-1}, which we assign to the stretch vibration of the methine group (ν_{CH}) of the FA molecule.[17] The signs of the $\mathrm{Im}[\chi^{(2)}]$ responses of the $\nu_{CH_3,SS}$ and $\nu_{CH_3,AS}$ vibrations of AA and the ν_{CH} of FA indicate that both molecules are oriented at the water surface with their CH bonds pointing toward the air phase.[21] For pure FA we observe that the band of the methine group (ν_{CH}) is shifted ∼15 cm^{-1} to higher frequencies in comparison to aqueous solutions of FA, in agreement with the results of a previous study of Johnson et al.[17] The $\mathrm{Im}[\chi^{(2)}]$ spectra for the AA and the FA solutions further show a broad band between 3000 and 3700 cm^{-1} that changes sign at a frequency of ∼3450 cm^{-1}. In previous intensity VSFG studies this response has been assigned to a low-frequency band centered at ∼3060 cm^{-1} and a high-frequency band centered at ∼3600 cm^{-1}, which were assigned to the OH stretch vibrations of strongly hydrogen-bonded OH groups of the carboxylic acids and to the OH stretch vibration of weakly hydrogen-bonded water molecules, respectively.[16] The $\mathrm{Im}[\chi^{(2)}]$ spectra in Figures 1a,b and 2a,b show that in fact there exists a single broad distribution of OH stretch frequencies that gives rise to two separate bands in the intensity VSFG spectrum because of the zero crossing at ∼3450 cm^{-1}. The broad OH response represents OH stretch vibrations of both acid and water molecules.[22]These vibrations are likely mixed and delocalized, but it is to be expected that the low-frequency OH vibrations are dominated by strongly hydrogen-bonded OH groups of the acid molecules while the high-frequency OH vibrations will show a dominant contribution of the OH stretch vibrations of weakly hydrogen-bonded water molecules.[16,22] The positive response near 3600 cm^{-1} shows a red shift with increasing acid concentration, which can be explained from the strengthening of the hydrogen bonds between the water and the acid molecules. At low carboxylic acid concentrations in Figures 1a and 2a an additional negative band centered at 3450 cm^{-1} is observed that vanishes with increasing acid concentration. This band is assigned to the OH stretch vibrations of hydrogen-bonded neat water molecules, in agreement with VSFG studies of the neat water surface.[21,23−25] For FA at low acid concentrations in Figure 2a additionally a sharp feature at 3700 cm^{-1} is observed, which vanishes when the acid concentration is increased. This band is assigned to the OH stretch vibrations of non-hydrogen-bonded OH groups of the neat water surface that stick out of the surface.[26,27]

To analyze the $\mathrm{Im}[\chi^{(2)}]$ quantitatively, we decompose the measured responses at different acid concentrations into several Lorentzian bands. For AA we decompose the $\mathrm{Im}[\chi^{(2)}]$ into four Lorentzian bands centered at 2935, 2970, 3060, and 3600 cm^{-1}, describing the symmetric ($\nu_{CH_3,SS}$) and antisymmetric ($\nu_{CH_3,AS}$) stretch vibration of the methyl group and the low- and high-frequency part of the OH stretch vibrations, respectively (Figure 1c,d). For FA we decompose the $\mathrm{Im}[\chi^{(2)}]$ spectra at different concentrations in three Lorentzian bands, centered at 2910, 3060, and 3600 cm^{-1}, representing the stretch vibration of the methine group (ν_{CH}) and the low- and high-frequency part of the OH stretch vibrations, respectively (Figure 2c,d). For both AA and FA we added an additional asymmetric Lorentzian curve centered at 3450 cm^{-1} to represent the response of the hydrogen-bonded OH stretch vibrations of the neat water surface. For FA we added further a narrow Lorentzian band centered at 3700 cm^{-1} representing the response of the OH stretch vibrations of non-hydrogen-bonded OH groups of the neat water surface. The $\mathrm{Im}[\chi^{(2)}]$ spectrum of the neat water surface in this frequency region can be found in the Supporting Information (Figure S1a). In the decomposition we keep the widths of all Lorentzian bands constant and allow only the amplitudes of the bands to change with the acid concentration. The bands of the symmetric and antisymmetric vibrations of the methyl group of AA are highly correlated, and we used a single parameter to represent their amplitudes in the fitting procedure.

https://doi.org/10.1021/acs.jpcb.1c09051
J. Phys. Chem. B 2022, 126, 270−277

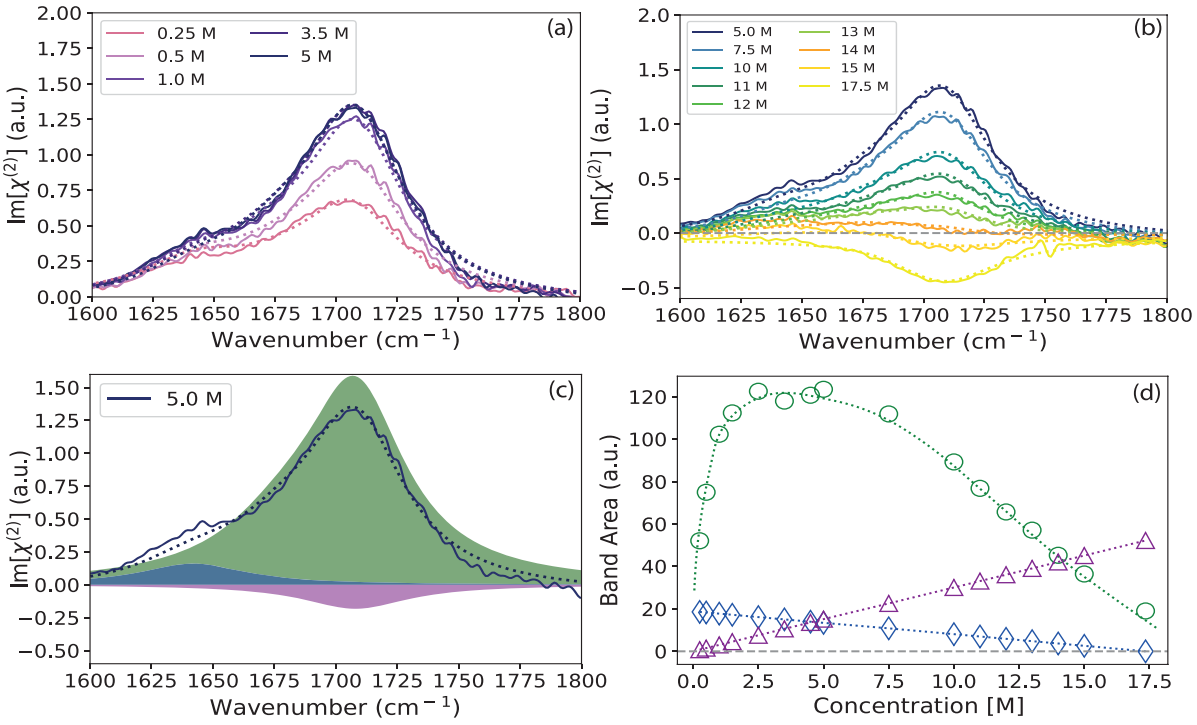

Figure 3. Im[$\chi^{(2)}$] spectra of aqueous solutions containing different concentrations of AA (a) in the range of 0.5−5 M and (b) in the range of 5−17.5 M (pure AA) in the frequency region of 1600−1800 cm^{-1}. (c) Decomposed spectra of AA with three Lorentzian bands centered at 1650, 1707, and 1712 cm^{-1} describing the water bending mode (blue), the dipolar response of the C═O vibration (green), and the quadrupolar response of the C═O vibration (magenta). (d) Absolute area of these bands extracted from the fitting procedure as a function of acid concentration.

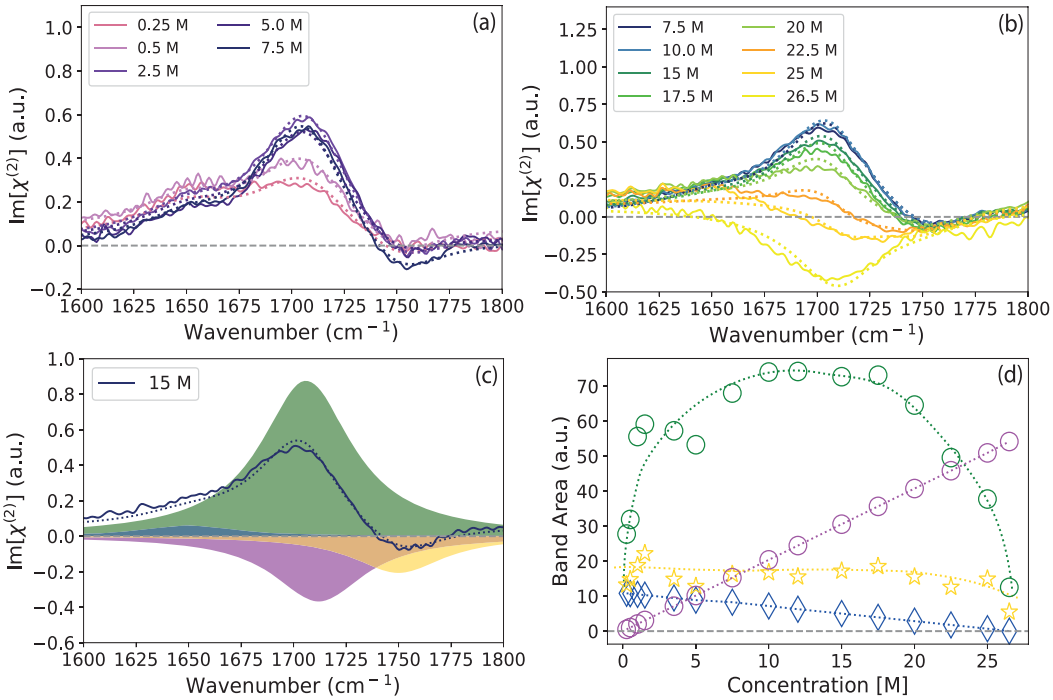

Figure 4. Im[$\chi^{(2)}$] spectra of aqueous solutions containing different concentrations of FA (a) in the range of 0.5−7.5 M and (b) in the range of 7.5−26.5 M (pure FA) in the frequency region of 1600−1800 cm^{-1}. (c) Decomposed spectra of FA with four Lorentzian bands centered at 1650, 1707, and 1712 cm^{-1} and the response of the linear FA dimers (yellow) describing the water bending mode (blue), the dipolar response of the C═O vibration (green), the quadrupolar response of the C═O vibrations (magenta), and the response of the linear FA dimers (yellow). (d) Absolute area of these bands extracted from the fitting procedure as a function of acid concentration.

The resulting fits of the Im[$\chi^{(2)}$] are shown in Figures 1a,b and 2a,b with dashed lines and are presented in more detail in the Supporting Information (Figures S2a−j and S3a−j). As an example, we show in Figures 1c and 2c the decomposition of the Im[$\chi^{(2)}$] spectrum of an AA and a FA solution with a concentration of 10 M.

https://doi.org/10.1021/acs.jpcb.1c09051
J. Phys. Chem. B 2022, 126, 270−277

In Figures 1d and 2d we present the areas of the vibrational modes extracted from the fitting procedure as a function of acid concentration. For the symmetric and antisymmetric vibrations of the methyl group of AA, the area shown is the sum of the absolute areas of the two bands. For both AA and FA we observe that the areas of the CH bands (magenta) increase with increasing concentration up to concentrations of 7.5 M for AA and 15 M for FA and then start to decrease. The initial increase of the areas of the CH bands can be well explained from the increasing surface coverage by the acid molecules. This interpretation is supported by surface tension measurements and calculations.[6,15,28] For acetic acid solutions the surface tension strongly decreases with increasing acid concentration, which shows that the concentration of acetic acid molecules at the surface is enhanced in comparison to its bulk contribution. The surface mole fraction of acetic acid can be obtained from the concentration dependence of the surface tension and accounting for the surface areas of the water and acetic acid molecules.[15] The response of the CH vibrations saturates at a higher acid concentration for FA than for AA, which can be explained from the fact that the FA molecules are less hydrophobic than the AA molecules and therefore less surface active. For the low-frequency OH band we observe a steep increase up to a concentration of 5 M for AA and 7.5 M for FA. This increase also follows from the increasing accumulation of acid molecules at the surface. This accumulation enhances the average strength of the hydrogen-bond interactions due to the strong hydrogen-bond-donating character of the acid hydroxyl group. In addition, the degree of orientation with respect to the surface normal of the strongly hydrogen-bonded OH groups will be enhanced with increasing concentration of acid molecules at the surface, as these acid molecules have a distinct preferential orientation of their OH groups toward the bulk. Above concentrations of 7.5 M for AA and 12 M for FA, the low-frequency OH band is observed to decrease with increasing acid concentration. The origin of this decrease will be discussed later. For both AA and FA the area of the high-frequency OH band (green) is constant up to a concentration of ∼5 M and then decreases until it completely vanishes for the pure acid. The fact that the area of the band remains constant up to ∼5 M does not mean that the number density of high-frequency OH oscillators remains constant. For concentrations up to ∼5 M the high-frequency OH band is also observe to shift to lower frequencies, which implies a strengthening of the hydrogen bonds of the OH groups. Hence, the constant area of this band while red-shifting in fact implies that the number density of high-frequency OH oscillators decreases. The high-frequency OH response is dominated by weakly hydrogen-bonded water molecules, and the decrease of the number density can thus be well explained from the decrease of the amount of water in the solution with increasing acid concentration.

To further enhance the understanding of the molecular properties at the solution surface we also studied the response in the frequency region of the C═O stretch vibration of AA and FA. Figures 3a and 4a show the experimental $\mathrm{Im}[\chi^{(2)}]$ spectra (measured in SSP polarization configuration) of aqueous AA and FA solutions at different concentrations in the frequency region of 1600−1800 cm^{-1}. For AA the concentration is ranging from 0.5 to 5 M AA and for FA from 0.5 to 7.5 M. For both AA and FA the $\mathrm{Im}[\chi^{(2)}]$ spectrum shows a positive band centered at 1707 cm^{-1} with a shoulder centered at 1650 cm^{-1}. The band at 1707 cm^{-1} increases with increasing acid concentration and is assigned to the C═O stretch vibration of the acid molecules. The increase of the vibrational band of the C═O group is similar to the increase of the response of the CH vibrations shown in Figures 1a,b and 2a,b. The positive sign of the $\mathrm{Im}[\chi^{(2)}]$ response of the C═O stretch vibration indicates that the positive charge of the C═O group is closer to the surface than the negative charge, which implies that the C═O group points with its oxygen atom toward the bulk.[14,29,30] This finding is consistent with the observation that the methyl group of AA and the methine group of FA are oriented toward the air. The $\mathrm{Im}[\chi^{(2)}]$ spectrum of the neat water surface shows a vibrational response centered at 1650 cm^{-1} (Figure S1b) that is assigned to the water bending mode. Therefore, we explain the shoulder at 1650 cm^{-1} that is observed in the spectra of Figures 3 and 4 to the response of the water bending mode.[11,12,17,31−33] The assignment is supported by measurements of AA and FA in D_2O solution that show that the band at 1650 cm^{-1} vanishes (Figures S4 and S5). With increasing acid concentration the band at 1650 cm^{-1} decreases due to the decrease in water content within the solution. For FA we observe an additional negative band centered at 1750 cm^{-1}, which we assign to the vibrational response of non-hydrogen-bonded carbonyl groups.[16,34−36] In Figures 3b and 4b we present $\mathrm{Im}[\chi^{(2)}]$ spectra of aqueous AA and FA solutions at even higher concentrations. The concentration of AA is ranging from 5 to 17.5 M (pure AA), and the concentration of FA ranges from 7.5 to 26.5 M (pure FA). We observe that in this concentration range the positive band of the C═O vibration decreases and changes sign.

To analyze the spectra quantitatively, we decompose the $\mathrm{Im}[\chi^{(2)}]$ spectra into Lorentzian bands. For AA we decompose the $\mathrm{Im}[\chi^{(2)}]$ into three Lorentzian bands at 1650, 1707, and 1712 cm^{-1} (Figure 3c,d). For FA we decompose the experimental $\mathrm{Im}[\chi^{(2)}]$ spectra into four Lorentzian bands (Figure 4c,d), representing the same responses as for AA and an additional band centered at 1750 cm^{-1}. We keep the widths of all Lorentzian bands constant and only allow the amplitude of the different contributions to change with acid concentration. The resulting fits are shown in Figures 3a,b and 4a,b with dashed lines and are presented in more detail in the Supporting Information (Figures S6a−j and S7a−j). As an example, we show in Figures 3c and 4c the fitted decomposition of the $\mathrm{Im}[\chi^{(2)}]$ of an AA solution at a concentration of 11 M and of an FA solution at a concentration of 15 M. In Figures 3d and 4d we present the areas of the vibrational modes extracted from the fitting procedure as a function of the acid concentration. With increasing acid concentration the area of the response of the C═O vibration at 1707 cm^{-1} (green) first increases, for AA up to a concentration of 2.5 M and for FA up to a concentration of 7.5 M. Increasing the concentration further leads to a decrease of this band. The decrease and vanishing of the positive response of the C═O vibrations at higher concentrations are in good agreement with the results of Johnson et al.[16] and can be explained by the formation of cyclic AA dimers.[16,37] Cyclic dimers are centrosymmetric and therefore do not show a dipolar vibrational SFG response. This formation of cyclic dimers also explains why we observed a decrease of the low-frequency OH band at concentrations >5 M for AA and >7.5 M for FA.

The positive C═O band not only decreases but even changes sign at concentrations >14 M for AA and >22.5 M for FA. This sign change can be well accounted for by including in the fitting a negative band centered at 1712 cm^{-1}, of which the amplitude increases with concentration. This band can be assigned to the quadrupolar response of the carbonyl vibration. This negative response becomes visible when the strong positive dipolar band

https://doi.org/10.1021/acs.jpcb.1c09051
J. Phys. Chem. B 2022, 126, 270−277

of the carbonyl vibration vanishes as a result of the formation of cyclic dimers. In a cyclic dimer the two carbonyl vibrations have a nearly perfect antiparallel arrangement, meaning that the dipolar response vanishes, thus leaving only the quadrupolar response of the C=O vibrations.[14] A detailed description of the quadrupolar response of molecular vibrations can be found in refs 10, 13, and 38−41. As the quadrupolar response of a particular vibration is not surface specific, its amplitude is expected to be proportional to the bulk concentration of that vibration. Therefore, in the fitting we assume that the amplitudes of the C=O band at 1712 cm^{-1} and the water bending mode at 1650 cm^{-1}, which also represent a quadrupolar response,[11,12] are directly proportional to the (bulk) concentrations of acid and water molecules, respectively. The area of the band at 1750 cm^{-1} is more or less constant throughout the whole concentration series. This band has been assigned to the response of non-hydrogen-bonded carbonyl groups[16,34−36] and is probably associated with linear FA dimers, which would imply that the concentration of linear dimers would be independent of the FA concentration.

In view of the observations in the frequency region of the C=O vibrations showing the formation of cyclic dimers at higher acid concentration, it is surprising that the responses of the CH vibrations of the methyl group of AA and of the methine group of FA do not strongly decrease at high acid concentrations. In cyclic acid dimers the CH groups of the acid molecules are arranged in an antisymmetric manner, which implies that the dipolar response of these vibrations is expected to vanish. There are two possible reasons why the response of the CH vibrations does not vanish due to the formation of cyclic dimers. The first is that even though the molecular structure of the cyclic dimers is centrosymmetric, the two aliphatic parts of the cyclic dimer are in quite different molecular environments, one part being much closer to the surface than the other part. Hence, on the molecular scale the symmetry of the methyl and methine may still be broken which would imply that the dipolar response of the CH vibrations does not vanish.[16] A second explanation is that the responses of the methyl and the methine groups show a quadrupolar bulk contribution that is not affected by the formation of cyclic dimers.[13,39] Here, a clear difference with the carbonyl vibration would be that for the CH vibrations the quadrupolar response is not of opposite sign to the dipolar response. As a result, for the CH vibrations the vanishing of the dipolar response only leads to a decrease of their $\mathrm{Im}[\chi^{(2)}]$ response, whereas for the C=O vibrations the vanishing of the dipolar response leads to a sign change of their $\mathrm{Im}[\chi^{(2)}]$ response.

The central frequency of 1712 cm^{-1} of the quadrupolar response of the carbonyl vibration is slightly higher than the central frequency of 1707 cm^{-1} of the dipolar response of this vibration. This difference may be due to the difference in hydrogen-bond configuration between a cyclic dimer and a hydrated monomer. However, this frequency difference may also result from the change of the frequency-dependent refractive index of the solution upon increasing acid concentration, as this will lead to a change of the Fresnel factors. To investigate a potential effect of the concentration dependence of the Fresnel factors, we modeled the sum-frequency response of the carboxyl group using the three-layer-model combined with the Lorentz model to estimate the refractive index of the interfacial layer (see Figure S8). A more detailed description of the model and the derivation of the Fresnel factors can be found elsewhere.[9,10,42] We find that at higher acid concentrations the Fresnel factors of the infrared light become frequency dependent, resulting in an enhancement of the high-frequency wing of the response of the carbonyl vibration. Therefore, the frequency of the maximum of the carbonyl vibration will shift to higher frequencies with increasing acid concentration, even if the intrinsic vibrational frequency itself would not change. In the fitting procedure the optimal frequency of maximum response of the dipolar component will be dominated by the spectra measured at low acid concentrations, while the optimal frequency of maximum response of the quadrupolar response is governed by the spectra measured at high acid concentrations. Hence, the difference of ∼5 cm^{-1} between the central frequencies of the fitted dipolar and quadrupolar responses can be due to the change of the Fresnel factors with acid concentration.

CONCLUSIONS

We performed heterodyne-detected vibrational sum frequency generation (HD-VSFG) measurements of aqueous acetic acid (AA) and formic acid (FA) solutions over a broad concentration range. In the frequency region from 2850 to 3700 cm^{-1} we find for both AA and FA solutions that the measured $\mathrm{Im}[\chi^{(2)}]$ spectra show an increase of the bands in the CH region with increasing acid concentration, which can be explained from the increase in surface coverage by the acid molecules. The OH vibrations of the acid and the water molecules give rise to a broad response between 3000 and 3700 cm^{-1}, of which the $\mathrm{Im}[\chi^{(2)}]$ response changes sign at a frequency of ∼3450 cm^{-1}. The amplitude of this band first increases with increasing acid concentration but starts to decrease for concentrations >5 M for AA and >7.5 M for FA, which can be explained from the formation of cyclic dimers. In cyclic dimers the vibrations of the acid monomers have a near-perfect antiparallel arrangement which cancels the dipolar sum-frequency generation response of these vibrations. In the frequency region from 1600 to 1800 cm^{-1} we observe a similar initial increase and subsequent decrease for the C=O stretch vibration of AA and FA at 1707 cm^{-1} as for the broad O−H stretch vibrational response of these acids, which can be explained again from the formation of cyclic dimers. We observe that the band at 1707 cm^{-1} decreases and even changes sign at high acid concentrations. This sign change can be well explained from the presence of a band at 1712 cm^{-1} which has a negative $\mathrm{Im}[\chi^{(2)}]$ response and that rises proportional to the bulk acid concentration. This band is assigned to the quadrupolar bulk response of the C=O stretch vibrations. The difference between the fitted frequency of the maximum quadrupolar response and the fitted frequency of maximum dipolar response may originate from the difference in hydrogen-bond configuration between a cyclic acid dimer and a hydrated monomer but can also be due to concentration-dependent Fresnel effects, as these effects enhance the high-frequency wing of the response at higher concentrations. Finally, we find that at high acid concentrations the vibrational responses of the CH vibrations saturate but do not strongly decrease. This indicates that in cyclic dimers the response of the CH groups of formic acid and acetic acid does not vanish because the two aliphatic parts of the cyclic acid dimer are in quite different molecular environments or because the response of the CH vibrations contains a quadrupolar contribution that is of the same sign as the dipolar response. The present observation of a quadrupolar bulk component in the VSFG responses of the C=O vibration, and possibly in the VSFG response of the CH vibrations, implies that the probing of liquids via VSFG spectroscopy of these

https://doi.org/10.1021/acs.jpcb.1c09051
J. Phys. Chem. B 2022, 126, 270−277

vibrations is likely not as surface specific as up to now has been assumed.

■ ASSOCIATED CONTENT

Supporting Information

The Supporting Information is available free of charge at https://pubs.acs.org/doi/10.1021/acs.jpcb.1c09051.

Figure S1: Im[$\chi^{(2)}$] spectrum of the neat water surface in the (a) 3 μm and (b) 6 μm regions; Figures S2 and S3: decomposition of the Im[$\chi^{(2)}$] of aqueous AA and FA solutions with different concentrations in the 3 μm region; Figures S4 and S5: Im[$\chi^{(2)}$] spectrum of aqueous AA and FA solutions with a concentration of 3.5 M in D_2O and H_2O; Figures S6 and S7: decomposition of the Im[$\chi^{(2)}$] of aqueous AA and FA solutions with different concentrations in the 6 μm region; Figure S8: modeling the effect of the Fresnel factors on the VSFG response of the carboxyl group for increasing concentrations (PDF)

■ AUTHOR INFORMATION

Corresponding Author

Huib J. Bakker − *Ultrafast Spectroscopy, AMOLF, 1098 XG Amsterdam, Netherlands;* orcid.org/0000-0003-1564-5314; Phone: +31 (0)20 754 7100; Email: H.Bakker@amolf.nl; Fax: +31 (0)20 754 7290

Authors

Carolyn J. Moll − *Ultrafast Spectroscopy, AMOLF, 1098 XG Amsterdam, Netherlands;* orcid.org/0000-0001-6041-5898

Jan Versluis − *Ultrafast Spectroscopy, AMOLF, 1098 XG Amsterdam, Netherlands*

Complete contact information is available at: https://pubs.acs.org/10.1021/acs.jpcb.1c09051

Notes

The authors declare no competing financial interest.

■ ACKNOWLEDGMENTS

This work is part of the research program of The Netherlands Organization for Scientific Research (NWO) and was performed at the research institute AMOLF. This project has received funding from the European Research Council (ERC) under the European Union's Horizon 2020 research and innovation program (grant agreement no. 694386)

■ REFERENCES

(1) Chebbi, A.; Carlier, P. Carboxylic Acids in the Troposphere, Occurrence, Sources, and Sinks: a Review. *Atmos. Environ.* **1996**, *30*, 4233−4249.

(2) Talbot, R. W.; Dibb, J. E.; Lefer, B. L.; Scheuer, E. M.; Bradshaw, J. D.; Sandholm, S. T.; Smyth, S.; Blake, D. R.; Blake, N.; Sachse, G. W.; et al. Large-scale distributions of tropospheric nitric, formic, and acetic acids over the western Pacific basin during wintertime. *Journal of Geophysical Resaerch* **1997**, *102*, 28303−28313.

(3) Fukuda, Y. Indoor Corrosion of Copper and Silver Exposed in Japan and ASEAN1 Countries. *J. Electrochem. Soc.* **1991**, *138*, 1238.

(4) Leygraf, C.; Wallinder, I. O.; Tidblad, J.; Graedel, T. *Atmospheric Corrosion*; John Wiley and Sons: Hoboken, NJ, 2016.

(5) Křepelová, A.; Bartels-Rausch, T.; Brown, M. A.; Bluhm, H.; Ammann, M. Adsorption of Acetic Acid on Ice Studied by Ambient-Pressure XPS and Partial-Electron-Yield NEXAFS Spectroscopy at 230 240 K Ade l a Kr e. *journal of physical chemistry. A* **2013**, *117*, 401−409.

(6) Álvarez, E.; Vázquez, G.; Sánchez-Vilas, M.; Sanjurjo, B.; Navaza, J. M. Surface tension of organic acids + water binary mixtures from 20°C to 50°C. *J. Chem. Eng. Data* **1997**, *42*, 957−960.

(7) Sugiyama, S.; Yoshino, T.; Kanahara, H.; Shichiri, M.; Fukushi, D.; Ohtani, T. Effects of acetic acid treatment on plant chromosome structures analyzed by atomic force microscopy. *Anal. Biochem.* **2004**, *324*, 39−44.

(8) Young, J. T.; Boerio, F. J. Surface-Enhanced Raman Scattering as an In-Situ Probe of Polyimide/Silver Interphases. *MRS Proc.* **1993**, *304*, 199.

(9) Shen, Y. R. *Fundamentals of Sum-Frequency Spectroscopy*; Cambridge University Press: Cambridge, 2016; pp 23−50, 91−97.

(10) Morita, A. *Theory of Sum Frequency Generation Spectroscopy*; Springer: Singapore, 2018; pp 1−13, 13−46, 151−200.

(11) Kundu, A.; Tanaka, S.; Ishiyama, T.; Ahmed, M.; Inoue, K. I.; Nihonyanagi, S.; Sawai, H.; Yamaguchi, S.; Morita, A.; Tahara, T. Bend Vibration of Surface Water Investigated by Heterodyne-Detected Sum Frequency Generation and Theoretical Study: Dominant Role of Quadrupole. *J. Phys. Chem. Lett.* **2016**, *7*, 2597−2601.

(12) Moll, C. J.; Versluis, J.; Bakker, H. J. Direct Evidence for a Surface and Bulk Specific Response in the Sum-Frequency Generation Spectrum of the Water Bend Vibration. *Phys. Rev. Lett.* **2021**, *127*, 116001.

(13) Mori, W.; Wang, L.; Sato, Y.; Morita, A. Development of quadrupole susceptibility automatic calculator in sum frequency generation spectroscopy and application to methyl C—H vibrations. *J. Chem. Phys.* **2020**, *153*, 174705.

(14) Wang, L.; Mori, W.; Morita, A.; Kondoh, M.; Okuno, M.; Ishibashi, T.-A. Quadrupole Contribution of CO Vibrational Band in Sum Frequency Generation Spectra of Organic Carbonates. *J. Phys. Chem. Lett.* **2020**, *11*, 8527−8531.

(15) Tyrode, E.; Johnson, C. M.; Baldelli, S.; Leygraf, C.; Rutland, M. W. A Vibrational Sum Frequency Spectroscopy Study of the LiquidGas Interface of Acetic Acid-Water Mixtures: 2. Orientation Analysis. *J. Phys. Chem. B* **2005**, *109*, 329−341.

(16) Johnson, C. M.; Tyrode, E.; Baldelli, S.; Rutland, M. W.; Leygraf, C. A Vibrational Sum Frequency Spectroscopy Study of the Liquid - Gas Interface of Acetic Acid - Water Mixtures: 1. Surface Speciation. *J. Phys. Chem. B* **2005**, *109*, 321−328.

(17) Johnson, C. M.; Tyrode, E.; Kumpulainen, A.; Leygraf, C. Vibrational sum frequency spectroscopy study of the liquid/vapor interface of formic acid/water solutions. *J. Phys. Chem. C* **2009**, *113*, 13209−13218.

(18) Shen, Y. R. Phase-Sensitive Sum-Frequency Spectroscopy. *Annu. Rev. Phys. Chem.* **2013**, *64*, 129−150.

(19) Moll, C. J.; Meister, K.; Kirschner, J.; Bakker, H. J. Surface Structure of Solutions of Poly(vinyl alcohol) in Water. *J. Phys. Chem. B* **2018**, *122*, 10722−10727.

(20) Strazdaite, S.; Versluis, J.; Backus, E. H. G.; Bakker, H. J. Enhanced ordering of water at hydrophobic surfaces. *J. Chem. Phys.* **2014**, *140*, 54711.

(21) Nihonyanagi, S.; Yamaguchi, S.; Tahara, T. Direct evidence for orientational flip-flop of water molecules at charged interfaces: A heterodyne-detected vibrational sum frequency generation study. *J. Chem. Phys.* **2009**, *130*, 204704.

(22) Moll, C.; Meister, K.; Versluis, J.; Bakker, H. Freezing of Aqueous Carboxylic Acid Solutions on Ice. *J. Phys. Chem. B* **2020**, *124*, 5201−5208.

(23) Pieniazek, P. A.; Tainter, C. J.; Skinner, J. L. Interpretation of the water surface vibrational sum-frequency spectrum. *J. Chem. Phys.* **2011**, *135*, 044701.

(24) Ishiyama, T.; Morita, A. Vibrational spectroscopic response of intermolecular orientational correlation at the water surface. *J. Phys. Chem. C* **2009**, *113*, 16299−16302.

(25) Nihonyanagi, S.; Kusaka, R.; Inoue, K. I.; Adhikari, A.; Yamaguchi, S.; Tahara, T. Accurate determination of complex χ (2) spectrum of the air/water interface. *J. Chem. Phys.* **2015**, *143*, 124707.

(26) Morita, A.; Hynes, J. T. A theoretical analysis of the sum frequency generation spectrum of the water surface. *Chem. Phys.* **2000**, *258*, 371−390.
(27) Du, Q.; Superfine, R.; Freysz, E.; Shen, Y. R. Vibrational spectroscopy of water at the vapor/water interface. *Phys. Rev. Lett.* **1993**, *70*, 2313−2316.
(28) Bagheri, A.; Alizadeh, K. How do temperature and chemical structure affect surface properties of aqueous solutions of carboxylic acids? *Colloids Surf., A* **2015**, *467*, 78−88.
(29) Okuno, M.; Yamada, S.; Ohto, T.; Tada, H.; Nakanishi, W.; Ariga, K.; Ishibashi, T. A. Hydrogen Bonds and Molecular Orientations of Supramolecular Structure between Barbituric Acid and Melamine Derivative at the Air/Water Interface Revealed by Heterodyne-Detected Vibrational Sum Frequency Generation Spectroscopy. *J. Phys. Chem. Lett.* **2020**, *11*, 2422−2429.
(30) Moll, C. J.; Versluis, J.; Bakker, H. J. Direct Observation of the Orientation of Urea Molecules at Charged Interfaces. *J. Phys. Chem. Lett.* **2021**, *12*, 10823−10828.
(31) Nagata, Y.; Hsieh, C. S.; Hasegawa, T.; Voll, J.; Backus, E. H.; Bonn, M. Water bending mode at the water-vapor interface probed by sum-frequency generation spectroscopy: A combined molecular dynamics simulation and experimental study. *J. Phys. Chem. Lett.* **2013**, *4*, 1872−1877.
(32) Ni, Y.; Skinner, J. L. IR and SFG vibrational spectroscopy of the water bend in the bulk liquid and at the liquid-vapor interface, respectively. *J. Chem. Phys.* **2015**, *143*, 014502.
(33) Vinaykin, M.; Benderskii, A. V. Vibrational sum-frequency spectrum of the water bend at the air/water interface. *J. Phys. Chem. Lett.* **2012**, *3*, 3348−3352.
(34) Spinner, E. Comment on 'A simple method for the matrix isolation of monomeric and dimeric carboxylic acids'. Possible implications of findings, in regard to liquid formic acid. *Spectrochim. Acta, Part A* **1999**, *55*, 1819−1825.
(35) Lim, M.; Hochstrasser, R. M. Unusual vibrational dynamics of the acetic acid dimer. *J. Chem. Phys.* **2001**, *115*, 7629−7643.
(36) Gantenberg, M.; Halupka, M.; Sander, W. Dimerization of Formic Acid-An Example of a "Noncovalent" Reaction Mechanism. *Chem.—Eur. J.* **2000**, *6*, 1865−1869.
(37) Bertie, J. E.; Michaelian, K. H. The Raman spectra of gaseous formic acid -h2 and -d2. *J. Chem. Phys.* **1982**, *76*, 886−894.
(38) Shiratori, K.; Morita, A. Theory of Quadrupole Contributions from Interface and Bulk in Second-Order Optical Processes. *Bull. Chem. Soc. Jpn.* **2012**, *85*, 1061−1076.
(39) Matsuzaki, K.; Nihonyanagi, S.; Yamaguchi, S.; Nagata, T.; Tahara, T. Vibrational Sum Frequency Generation by the Quadrupolar Mechanism at the Nonpolar Benzene/Air Interface. *J. Phys. Chem. Lett.* **2013**, *4*, 1654−1658.
(40) Yamaguchi, S.; Shiratori, K.; Morita, A.; Tahara, T. Electric quadrupole contribution to the nonresonant background of sum frequency generation at air/liquid interfaces. *J. Chem. Phys.* **2011**, *134*, 184705.
(41) Shen, Y. R. Revisiting the basic theory of sum-frequency generation. *J. Chem. Phys.* **2020**, *153*, 180901.
(42) Wang, L.; Murata, R.; Inoue, K.-i.; Ye, S.; Morita, A. Dispersion of Complex Refractive Indices for Intense Vibrational Bands. II. Implication to Sum Frequency Generation Spectroscopy Published as part of The. *J. Phys. Chem. B* **2021**, *125*, 9804−9810.

https://doi.org/10.1021/acs.jpcb.1c09051
J. Phys. Chem. B 2022, 126, 270−277